

Description of Shale Pore Fracture Structure Based on Multi-Fractal Theory

LI Jinch^[a]; ZHAO Wanchun^{[b],*}; LIU Siqi^[a]

^[a]School of Earth Sciences, Changjiang University, Wuhan, China.

^[b] Northeast Petroleum University, China.

* Corresponding author.

Supported by Heilongjiang General Undergraduate Colleges and Universities Young Innovative Talents Training Plan (Grant No.UNPYSCT-2016084), Natural Science Foundation of Heilongjiang Province of China(Young Scientists) (Grant No.QC2017043),The 9th special China Postdoctoral science Foundation projects (Grant No.2016T90268),China Postdoctoral Foundation (Grant No.2018M630335), Key Young Project of Northeast Petroleum University “National Foundation” Cultivating foundation (Science) 2017. Natural Science Foundation of Heilongjiang Province of China (YQ2019E007).

Abstract

In order to describe the shale-fissure's structure and distribution accurately, this paper combines with complex features of shale rock mass' multilevel micro-scale fissure network, putting forward that utilizing the multi-fractal method to describe the distribution of fissures with different dimensions. By choosing some oil field's block shale samples, obtain the fissure distribution characteristics by CT scanning and calculate with the multi-fractal theory, the results show that the shale rock mass' fissure distribute in a multiple-fractal regularity. The study results lay a solid foundation of subsequent press shale fissure network's formation and description.

Key words: Shale rock; multi-fractal; CT scanning; fracture distribution

1. INTRODUCTION

A accurate description of the shale fissure's structure and distribution features is the key in the study of shale fracturing micro-crack evolution. Due to the complexity of shale rock mass fissure's distribution, shale fissure develop, with poor connectivity, is mostly filled by calcium and clay mineral. The fissure's size is complex, which range from nanoscale to millimeter size, belonging to the typical multilevel fissure system, and usually forming fissure group intensively, and natural fissure constitutes the natural fissure network.

To describe the shale rock mass' complex natural fracture, some scholars put forward different research methods. Article (Kang, Zhao & Jing, 1995; Shen, Zhao, & Zhu, 1955; Zhao, Wang, & Duan, 2002) carried on the statistics of the fracture's trace amount's distribution. It shown that the trace amounts distribute in fractal regularity, but it didn't explain the fracture surface's distribution regularity inside rock mass. Feng Zengchao, Zhao Yangsheng and some other schloars (2005) proved that the fracture surface's amount subjects to 3D fractal distribution use the computer simulation of numerical test method and obtained the basic relations of fracture surface's fractal dimension and fractal distribution's initial value as well as the fractal parameter. Katz, etc (1985) analyzed pore structure inside the porous medium by using the theory of fractal geometry, it was concluded that the pore space and pore interface of porous medium all have fractal structure. Hildgen ect. (1997) applied fractal theory to the measurement of heterogeneous porous media macro-porosity, and established the relations of fractal dimension and porous media's porosity. Jia Fenshu (1995) used image processing technology such as the determination of sandstone pore structure fractal dimension method, proposed the sandstone pore structure fractal scale's lower limit. He Wei ect. (2000) proposed research methods which using the pore fractal dimension to analyze the hole wall's roughness and pore size distribution's inhomogeneous degree based on the fractal theory. Tang Hongqi ect (Tang & Tang, 2004) discussed and analyzed on the sandstone core's fractal characteristic, she also points out that the fractal dimension has the characteristics of integrity and good correlation. Ghosh and Jaak J K Daemen (Zhang, 2013) depicted the joint characteristic of some open ore deposit's four rock-face in AZ Arizona by using the joint

† Received 2 September 2019 Accepted 16 November 2019 Published online 26 December 2019

Li, J. C., & Liu, S. Q. (2019). Description of Shale Pore Fracture Structure Based on Multi-Fractal Theory. *Advances in Petroleum Exploration and Development*, 18(1), 1-9. Available from:<http://www.cscanada.net/index.php/aped/article/view/11342>
DOI: <http://dx.doi.org/10.3968/11342>

fissure's fractal dimension; Thompson, A. H., Katz, A. J. et. (Bird, et al, 2006) faceted the rock crystalline grain's micro size quantitatively by using fractal geometry; Peng Ruidong et. (2011) proposed fractal dimension calculation based on pore structure's CT gray image; Yu Boming et. (Shi & Fan, 2002) and some foreign scholars (Karacan, 2003; Pitchumani & Ramakrishnan, 1999; Fomin, et al, 2011; Ramakrishnan & Pitchumani, 2000; Stach, et al, 2001) established the relationship between hole medium pore structure fractal characteristics and the permeability, relative permeability, and deduced a fractal model of fluid flow in different porous media's diffusion and heat conduction process, and had embarked on the study of multifractal structure characteristics.

Combining with shale rock mass' multilevel micro-scale fracture network's complex features, this paper puts forward describing the distribution of fissures with different dimensions by utilizing the multifractal method. By choosing some oil field block's shale samples, the paper obtains the fissure distribution characteristics by CT scanning, calculates with the multifractal theory. The results show that the shale fracture distribute with multiple fractal law. The study results lay a solid foundation of subsequent press shale fissure network's formation and description.

2. SHALE ROCK MASS FRACTURE DISTRIBUTION FEATURE'S 3D BULIDING

Obtain a set of two-dimensional slice image sequence by CT scans, after a 2D image processing of rock grain, pore space and fluid distribution information, it finishes 2D image to 3D image's conversion by 3D reconstruction so as to realize 3D visualization. After two-dimensional images is segmented, a set of continuous 2D image align, constitutes a three-dimensional data field. Now there are two mainly 3D reconstruction methods, the one is based on surface rendering and the other one is based on volume rendering, the most basic method to represent 3D object's shape is the former one; it can get comprehensive information about the three-dimensional objects. Surface rendering method's computation is small, and volume rendering method's computation is relatively large.

Longitudinal cutting scans the experiments core by the rock cutting system, transmits the single cutting rock mass in the standard form image to the computer image processing system. Computer processing system conducts grid subdivision of single core image, and marks coordinates, the mark principle is: assumed the core image's size is $L_0 \times L_0$, dividing the image into a square grid, which side length is $L * L$. The first grid coordinate of any grid profile is set to $(0, 0)$, then any grid coordinates within the grid is (m, n, k) , $m, n = 1, 2, \dots, L_0 / L$, k is the number of rock mass cut on the longitudinal, $k = 1, 2, \dots, H/h$, H is the total thickness of rock mass, h is the thickness of cutting unit on longitudinal.

Gray scale scan in core image. If any grid (m, n, k) is dominated by pore, pore length $r < L$, then the grid is given vector-valued represented as $[m, n, k, 1]$. If we don't consider bending fracture within the grid, and fissure drop in grid unit of the grid, and the grid fissure length meets $L \leq l \leq \sqrt{3} L$, then the grid is consider as a fissure unit, the grid is given by vector-valued $[m, n, k, 1]$. If the grid's space is occupied by a rock matrix, the grid is given by vector-valued $[m, n, k, 0]$, in which m and n are any grid point coordinates.

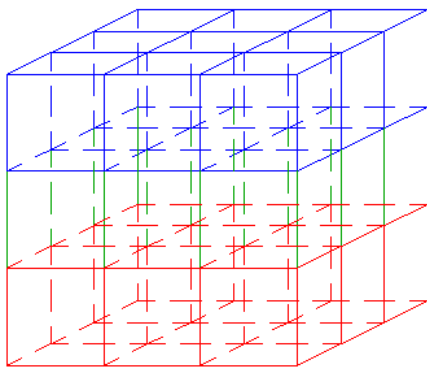


Figure 1: Rock mass 3-D structure meshing picture

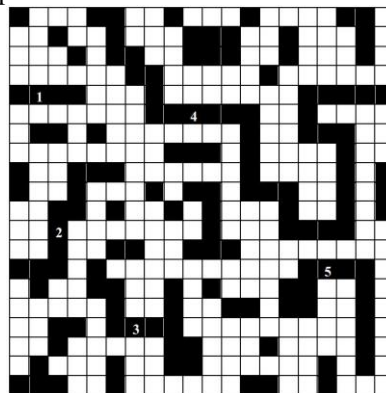


Figure 2: Rock mass pores and fractures distribution characteristics picture

Scanning all the rock mass's subdivision of the image, getting the whole rock mass pore fracture and the rock matrix's 3D vector representation is:

$$\begin{array}{l}
 \text{Rock matrix:} \\
 \begin{bmatrix} 1 & 1 & 1 & 0 \\ M & M & M & M \\ m & n & k & 0 \\ M & M & M & M \\ \frac{L_0}{L} & \frac{L_0}{L} & \frac{H}{h} & 0 \end{bmatrix}
 \end{array}
 \begin{array}{l}
 \text{pole:} \\
 \begin{bmatrix} 1 & 1 & 1 & 1 \\ M & M & M & M \\ m & n & k & 1 \\ M & M & M & M \\ \frac{L_0}{L} & \frac{L_0}{L} & \frac{H}{h} & 1 \end{bmatrix}
 \end{array}
 \begin{array}{l}
 \text{fissure:} \\
 \begin{bmatrix} 1 & 1 & 1 & -1 \\ M & M & M & M \\ m & n & k & -1 \\ M & M & M & M \\ \frac{L_0}{L} & \frac{L_0}{L} & \frac{H}{h} & -1 \end{bmatrix}
 \end{array}$$

Get connection group's characteristics by the method of addressing path, assume that both the grid which filled with the pore is disconnected, when a crack (or matrix) unit around is connected with at least a crack (or matrix) unit, the pore unit, matrix units and fracture units in grid's 1, 0, -1 distribution, superpose vector-valued of pores and fractures according to the law that $1 + 1 = 1$, $1 + 0 = 1$, $1 + (-1) = 1$, $0, 0 = 0$, $1 + 0 = 1$, $1 + (-1) = 1$, and finally formed the hole fissure coexistence's vector-valued.

For block shale sample scanning and image processing, the image analysis shows that the block shale pore fissure structure has certain multi-fractal, and draw the corresponding multi-fractal spectrum. Extract spectrum's width of fracture pore fissure structure from multi-fractal spectrum, the maximum and asymmetry degree curve of singular spectrum curve three main characteristic parameters. Through the analysis, three characteristic parameters can be used as the basis for determine shale pore fissure structure characteristics, and provides a new thought and method for the follow-up study of shale fracture structure.



Figure 3: Natural shale core sample machine



Figure 4: Sky scan 1172 high resolution CT

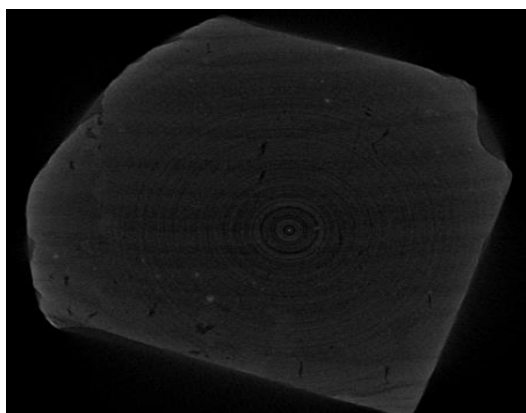
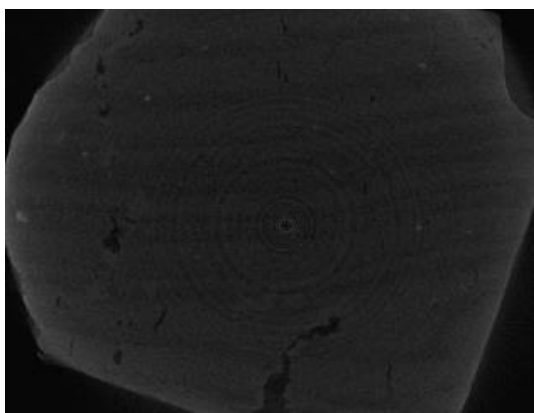


Figure 5: Fracture distribution picture of block 1 after CT scanning

First, select the SEM scanning of the S1 sample shown in Figure 5, and use the MATLAB image processing function for shale core scanning image of binarization, edge detection and extraction, the obtained results as shown in Figure 6 and Figure 7.

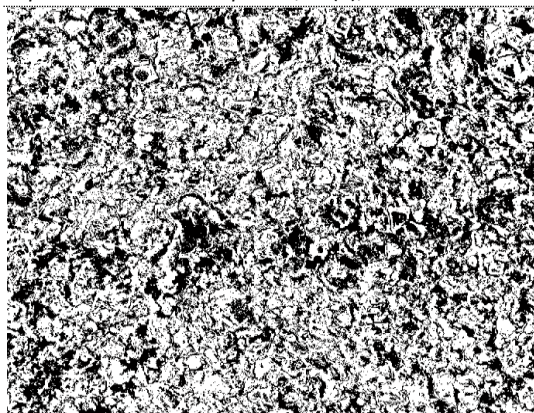


Figure 6: The characteristic line of core hole fracture structure

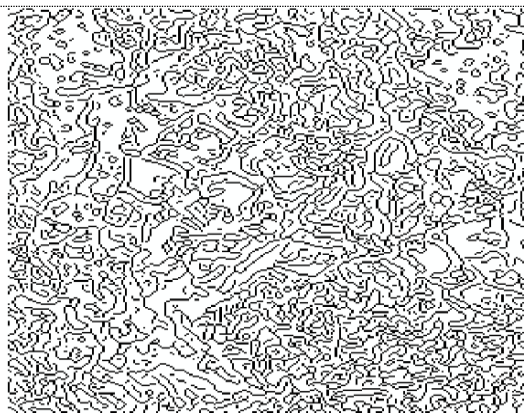


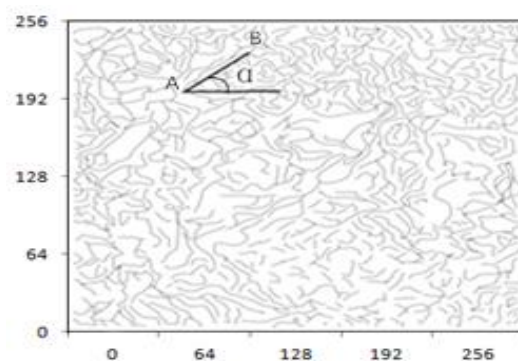
Figure 7: Edge detection of the fracture structure

Characteristic Line

The edge of Figure 4 is refined by hand by using the drawing board in Windows, and the initial simulation diagram of the shale core hole fracture structure is obtained as shown in Figure 8(a). Then the initial simulation map is converted into a pixel value of 256*256 bitmap (255 white background area, 0 of the point of the texture) in matlab, that is, the final simulation of the texture as shown in Figure 8 (b). Set up the Cartesian coordinates to determine the tilt angle of each curving line. When the scale is small to a certain extent, the curving part can approximately be straight segment, so the tilt angle of curving segments can be equivalent to the straight one. As is shown in Figure 8(b), the angle represents the angle between the crack AB and the horizontal.



(a) Untreated initial simulation



(b) Simulation after treatment figure

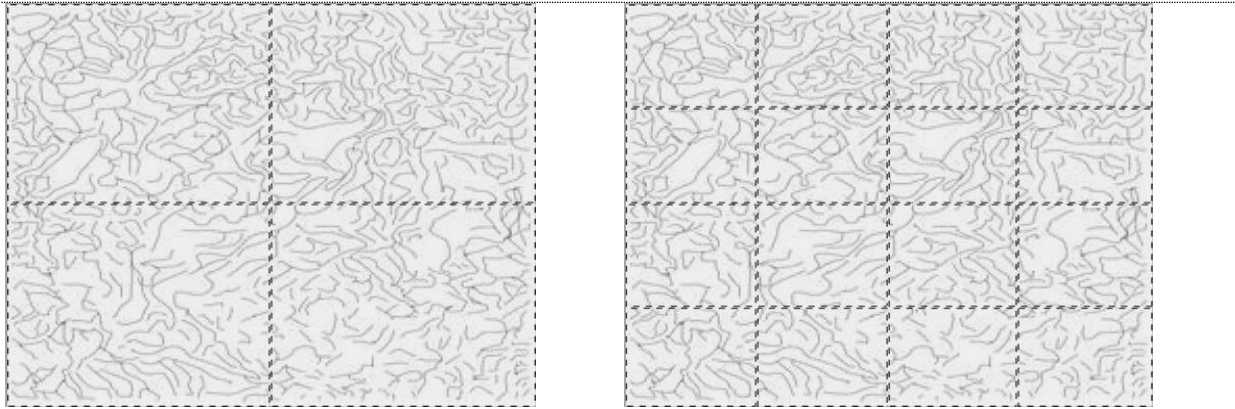
Figure 8: Simulation of shale pore fracture structure

3. MULTI-FRACTAL THEORY AND ITS ALGORITHM

3.1 Shale Pore Fracture Structure Simulation

Box counting method is used to dealing with the simulation of the shale hole fracture structure, that is, the image is divided into square sub area whose length is equal to the division scale λ . we assume that the length of each unit is 256 pixel value, so the smallest size of the division scale is 1/256.

However, we can only get some isolated pixels, not the little curving segment, so division scale λ should be suitable to extract enough little curving line. In this passage, the scale we take is 1/2, 1/3, 1/4, 1/5, 1/6, 1/8, 1/12, 1/16, so the corresponding pixel value of each scale is 128, 85, 64, 51, 42, 32, 23, 16. The images in Figure 9(a) and (b) represent the segmentation of the fracture structure simulation diagram (Figure 8) when the division scale is 1/2 and 1/4.



(a) When the division scale λ is 1/2, the region is divided into 4 equal square sub regions (b) When the division scale λ is 1/4, the region is divided into 16 equal square sub regions

Figure 9: Segmentation of the simulation of shale pore fracture structure

In each small square area, we define the sum of the title angle of every small curving line is $\theta_i(\lambda)$, which depends on the size of the division scale λ . For each identified division scale λ . The sum of all the title angles of all little curving lines in the shale fracture simulation is put the entire title angle $\theta(\lambda)$ together:

$$\theta(\lambda) = \sum_i \theta_i(\lambda) \quad (1)$$

The probability density distribution function $p_i(\lambda)$ corresponding to each small square area is obtained.

$$p_i(\lambda) = \frac{\theta_i(\lambda)}{\theta(\lambda)} \quad (2)$$

From the formula, we can see that the size of $p_i(\lambda)$ depends only on i and λ .

3.2 Multi-Fractal Theory

The distribution function $x_q(\lambda)$ is determined according to the probability density distribution function $p_i(\lambda)$.

$$x_q(\lambda) = \sum_i (p_i(\lambda))^q \quad (3)$$

The purpose of defining the partition function is to describe the function of probability density distribution

function $p_i(\lambda)$. We determine whether the power law relation $x_q(\lambda) = \sum (p_i(\lambda)) \propto \lambda^{\tau(q)}$ is established according to

whether there is a linear relationship between the double logarithm curve $\log x_q(\lambda) - \log \lambda$. We can get the quality

index function $\tau(q)$ according to the double logarithm relation:

$$\tau(q) = \lim_{\lambda \rightarrow \infty} \frac{\log x_q(\lambda)}{\log(\lambda)}, (\lambda \rightarrow 0) \quad (4)$$

If $\tau(q)$ is a linear function about q , it is indicated that the pore structure of shale is distributed as a single fractal; If there is no linear relationship between $\tau(q)$ and q , it shows that the pore structure distribution of shale has multi-fractal properties, and the fractal dimension is the generalized one. By means of the corresponding transformation, we can determine the relationship between the mass index function $\tau(q)$ and the generalized fractal dimension $D^{(q)}$ is

$$\begin{cases} \frac{\tau(q)}{q-1} (q \neq 1) \\ \tau'(q) (q = 1, \text{ and } \tau(q) \text{ is different}) \end{cases} \quad (5)$$

In particular, $D^{(0)}$ is the capacity dimension. In the non scale region, the probability measure $p_i(\lambda)$ has the scaling relation as following:

$$p_i(\lambda) \propto \lambda^\alpha \quad (6)$$

where α_i is the singular scale index. The range of α in the image is from α_{\min} to α_{\max} .

If the number of boxes with the same identity $\alpha^{(i)}$ is $N\alpha^{(i)}$, the scaling relationship existing in the non scale area is:

$$N_{\alpha}(\lambda) \sim \lambda^{-f(\alpha)} \quad (7)$$

Here the $f(\alpha)$ in which the fractal dimension of subset is identified by α , and divided into a series of subset fractal features in complex fractal, is called the multi-fractal spectrum or singular spectrum.

When $\tau(q)$ and $f(\alpha)$ are different, the generalized fractal dimension $D^{(q)}$ and multi-fractal spectrum $f(\alpha)$ meet the Legendry transform:

$$\begin{cases} \alpha(q) = \frac{d\tau(q)}{dq} \\ f(\alpha) = q \bullet \alpha(q) - \tau(q) \end{cases} \quad (8)$$

According to the Legendre transform, we can know that if the object of the study is a single fractal, the function is a certain value, and if it is the multi-fractal, the function is generally a single peak curve, and the interval meet that $f(\alpha) \geq 0$ is the range of α ranging from α_{\min} to α_{\max} . It is satisfied the following relationship:

$$f(\alpha_{\min}) = f(\alpha_{\max}) = 0 \quad (9)$$

There must exists an α_0 between α_{\min} and α_{\max} , which can establish the relationship that $f_{\max} = f(\alpha_0)$. Then we can use three parameters to describe the multi-fractal degree of shale pore structure:

The maximum value of multi-fractal:

$$f_{\max} = f(\alpha_0), \alpha_0 \in [\alpha_{\min}, \alpha_{\max}] \quad (10)$$

The width of multi-fractal spectrum:

$$W = \alpha_{\max} - \alpha_{\min} \quad (11)$$

The f_{\max} can be obtained in the vicinity of $\alpha = \alpha_0$, and with the Minimum quadratic fitting method, we get the quadratic function:

$$f(\alpha) = A(\alpha - \alpha_0)^2 + B(\alpha - \alpha_0) + C \quad (12)$$

We assume that α_L is the left width of the singular spectrum and α_R is the right width, so the formula $B = \alpha_L - \alpha_R$ represents the asymmetric degree of the multi-fractal spectrum. When $B = 0$, the multi-fractal spectrum is symmetric; when $B > 0$, the peak value of multi-fractal spectrum is to the left; when $B < 0$, the peak value of multi-fractal spectrum is to the right. Generally speaking, when f_{\max} is bigger, the width of multi-fractal spectrum is greater and the symmetry of the multi-fractal spectrum is better, multi-fractal character is presented well. Therefore, the physical meaning of $f(\alpha)$ is a measure of the complexity, the degree of irregularity and the degree of inhomogeneity on the fractal structure. In the actual calculation, we generally use the following formula to calculate the spectral function.

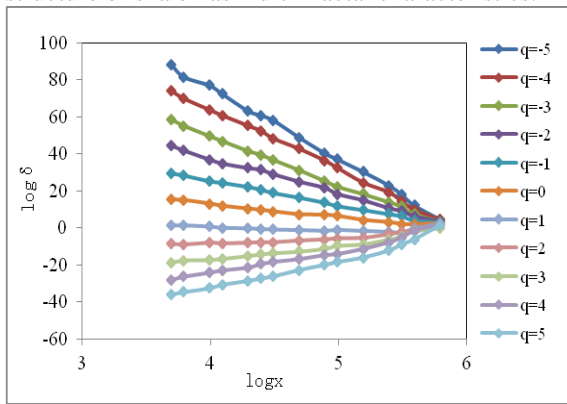
4. EXPERIMENTAL RESULTS AND ANALYSIS

According to the related formula and calculation method, the paper extracts the sum of all ditty line tilt angle corresponding to λ in each small square region, and then calculate the probability distribution function corresponding to every λ . we choose the range of q from -5 to 5, then obtain the m.files of double logarithmic function, partition function, mass index function, the generalized dimension function and multi-fractal spectrum function through the matlab program and calculated them. As shown in Figure 9, there are 11 double logarithmic curve diagrams which respectively correspond to the $q = -5, -4, -3, -2, -1, 0, 1, 2, 3, 4, 5$. It can be seen from the figure that the curves show a linear relationship between the rules, indicating that the relationship between q and x to

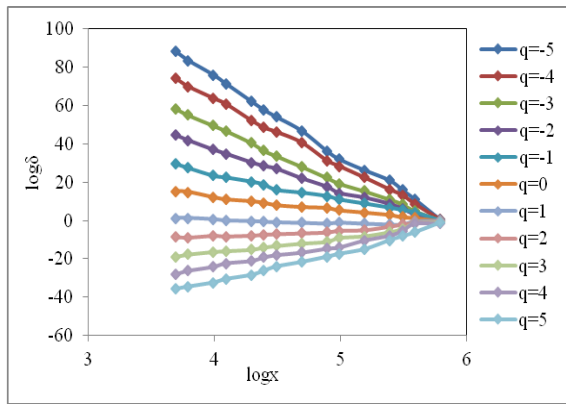
meet the power law relationship of $x_q(\lambda) = \sum (p_i(\lambda)) \propto \lambda^{\tau(q)}$.

This shows that the pore structure of shale in the range of the rules has the characteristic of scale-free, that is to say that the distribution of the pore structure of shale has fractal characteristics, According to the definition of $\tau(q)$, we can get the quality index function diagram as shown in Figure 10. As we can see from the graph, $\tau(q)$ is

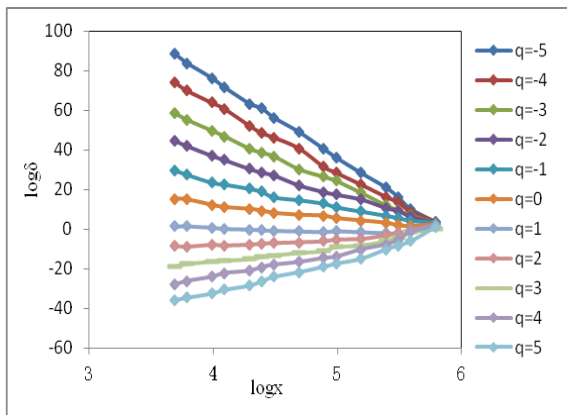
a convex function, that is, there is a nonlinear relationship between q and $\tau(q)$, which indicates that the pore structure of shale has multi-fractal characteristics.



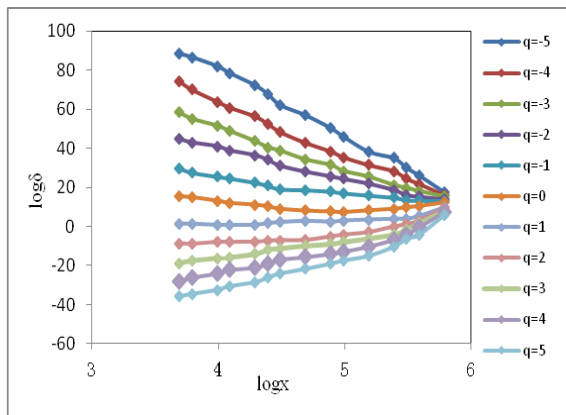
(a) Fracture length 0-0.2cm



(b) Fracture length 0.2-0.4cm



(c) Fracture length 0.4-0.6cm



(d) Fracture length 0.6-0.8cm

Figure 10: $\text{Log } x \sim \text{Log } \delta$ curve

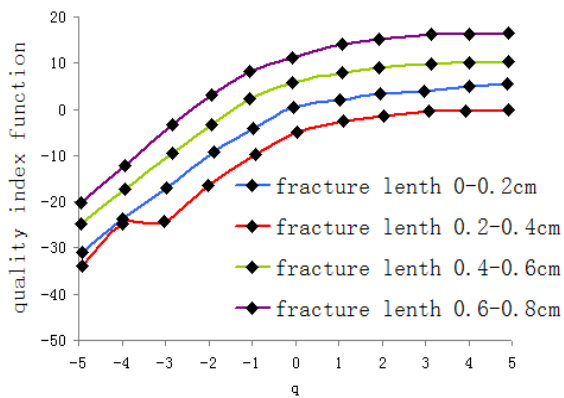


Figure 11: $\tau(q) \sim q$ Curve

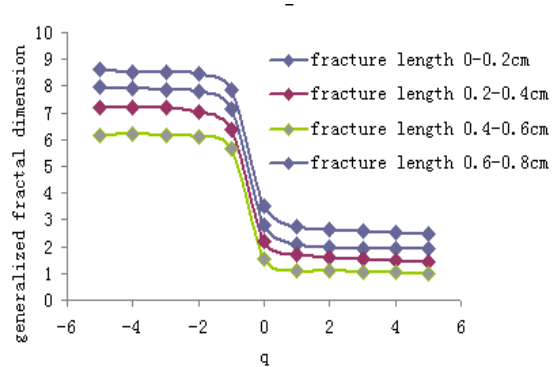


Figure 12: $D(q) \sim q$ Curve

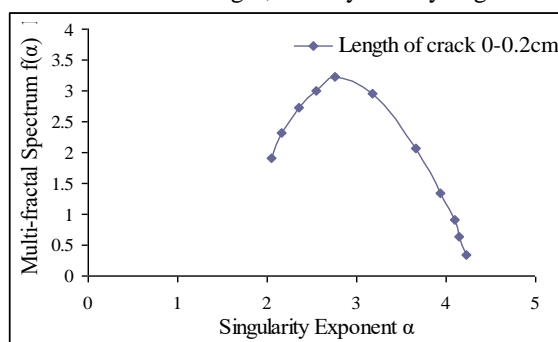
Based on Legendre transformation, obtain the generalized fractal dimension $D(q)$ diagram, we can get from $D(q) \sim q$ figure that when $q=0$, crack capacity dimension $D(0)=2.7945$. It can be obtained through calculation that when $\alpha_{\max}=4.2314$,

$\alpha_{\min}=2.0456$, $\alpha_0=3.1699$, the multifractal spectrum function obtains the peak, you can get $f_{\max}=f(\alpha_0-3.2167)$. Therefore, different length of cracks in each samples of important multifractal parameters is shown in Table 1:

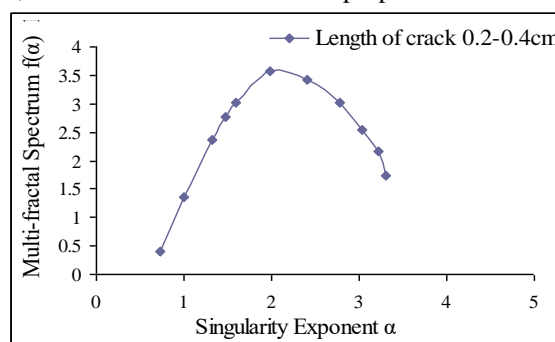
Table 1
Shale samples multifractal parameters calculation results

Rock samples	Rock samples			
	0-0.2cm	0.2-0.4cm	0.4-0.6cm	0.6-0.8cm
α_{max}	4.2314	3.3121	3.1762	3.8918
α_{min}	2.0456	0.7312	1.3145	0.6124
W	2.1858	2.5809	1.8617	2.2794
f_{max}	3.2167	3.5718	3.0821	3.6321
B	-0.7733	-0.0791	-0.0541	-0.1698

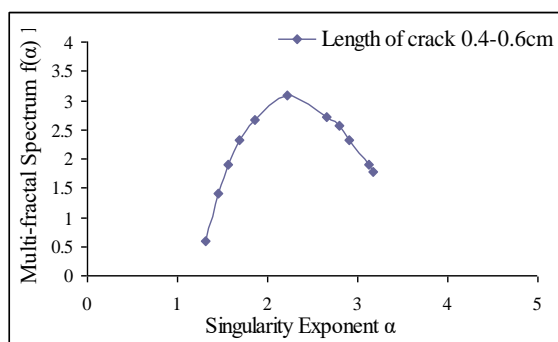
Through the above data we can see, two rock sample's hole fissure structure singular spectrum width and the maximum value is larger, and asymmetry degree is obvious, all have obvious multifractal properties.



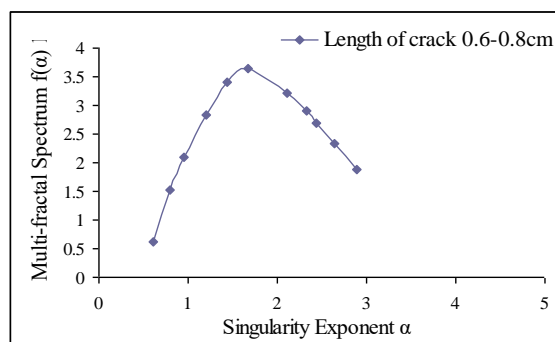
a) Fracture length 0-0.2cm



(b) Fracture length 0.2-0.4cm



(c) Fracture length 0.4-0.6cm



(d) Fracture length 0.6-0.8cm

Figure 13: Multi-ractal spectrum of rock mass fracture distribution characteristics (Sample 1)

The multifractal spectrum of different crack length $f(\alpha)-\alpha$ as shown in Figure 12, rack which length is 2-0.2cm has a minimum spectral width, while 0.6-0.8 cm has the maximum spectral width, micro-fracture with length of 0 to 0.2 cm distribute more uniform , 0.6 -0.8 cm distribute uneven, the smaller cracks are evenly distributed in the reservoir, and larger cracks concentration distribution in the reservoir, which is associated with the mineral composition and brittle characteristics of reservoir; Calculate, crack with 0-0.2 cm length's $\Delta f_{0-0.2}(\alpha) > 0$, other crack $\Delta f(\alpha) < 0$, show that cracks which with 0-0.2 cm length take a large proportion in the reservoir.

CONCLUSION

By CT scanning method, the measure the different scales of fracture in shale, the crack is classified according to the different scale, the study shows that the cracks of block scale can be divided into four grades: 0-0.2 cm, 0.2-0.4 cm, 0.4-0.6 cm, 0.6 -0.8 cm.

Established a method to describe the multifractal of shale rock mass fracture distribution, by choosing the actual core of A block, by calculate multifractal spectrum function of shale rock mass, the results prove that shale rock mass fracture distribution has multifractal characteristics. Micro-fracture with length of 0 to 0.2cm distribute more uniform , 0.6 -0.8cm distribute uneven, cracks which with 0-0.2cm length take a large proportion in the reservoir.

REFERENCES

- Bird, N., Diaz, M. C., Saa, A., et al. (2006). Fractal and multifractal analysis of pore-scale images of soil. *Journal of Hydrology*, 322, 211-219.
- Feng, Z. C., Zhao, Y. S., & Wen, Z. M. (2005). Study on 3D fractal distribution law of the surface number in rock mass. *Chinese Journal of Rock Mechanics and Engineering*, 24, 601-609.
- Fomin, S. A., Chugunov, V. A., Hash, I., & Da, T. (2011). Non-Fickian mass transport in fractured porous media. *Advances in Water Resources*, 34, 205-214.
- He, W., Zhong, F. X., He, C. Z., et al. (2000). A research and application of reservoir rock's the fractal structure. *Natural Gas Industry*, 20.
- Hildgen, P., Nekka, F., Hildgen, F., et al. (1997). Macroporosity measurement by fractal analysis. *Physica A*, 234, 593-603.
- Jia, F. S., Shen, P. P., & Li, K. W. (1995). Study on the fractal characteristics of sandstone pore structure and its application. *Fault-Block Oil and Gas Field / Fault-Block Oil Gas Field*, 2, 16-21.
- Kang, T. H., Zhao Y. S., & Jing, Z. M. (1995). Fractal study of crack scale distribution in coal mass. *Journal of China coal Societ*, 20, 393-398.
- Karacan, C. (2003). A fractal model for predicting permeability around perforation tunnels using size distribution of fragmented grains. *Journal of Petroleum Science and Engineering*, 40, 159-176.
- Katz, A. J., & Thompson, A. H. (1985). Fractal sandstone pores, Implications for conductivity and pore formation. *Phys. Rev. Lett.*, 54, 1325-1328.
- Peng, R. D., Yang, Y. C., Bian, Y., et al. (2011). Computation of fractal dimension of rock pores based on gray CT images. *Chinese Sci Bull*, 56, 2256-2266.
- Pitchumani, R., & Ramakrishnan, B. (1999). A fractal geometry model for evaluating permeabilities of porous preforms used in liquid composite molding. *International Journal of Heat and Mass Transfer*, 42, pp.2219-2232, 1999.
- Ramakrishnan, B., & Pitchumani, R. (2000). Fractal permeation characteristics of preforms used in liquid composite molding. *Polymer Composites*, 21, 281-296.
- Shen, J., Zhao, Y. S., & Zhu, E. S. (1955). Fractal distribution for rock mass in fractures for rock mass in high slopes and its application to the lock of Three Gorges. *Chinese Journal of Geo-technical Engineering*, 20, 97-100.
- Shi, M. H., & Fan, H. (2002). Fractal model of porous medium's heat conduction. *Journal of Thermal Science and Technology*, 1, 28-31.
- Stach, S., Cybo, J., & Chmiela, J. (2001). Fracture surface- fractal or multifractal. *Materials Characterization*, 26, 163-167.
- Tang, H. Y., & Tang, R. Q. (2004). A study on pore structure's fractal characteristics of sandstone core. *Journal of University of Science and Technology of China*, 34, 69-75.
- Zhang, B. (2013, April). *A fractal research on Yao copper sandstone mechanical and acoustic emission characteristic and damage rule*. A graduate student's thesis of Kunming University of Science and Technology.
- Zhao, Y. S., Wang, X. H., & Duan, A. L. (2002). Unsymmetry of scale transformation of rock mass anisotropy. *Chinese Journal of Rock Mechanics and Engineering*, 21, 1594-1597.